Fig. 4 HCV-Core and NS5A proteins are the proteins that contribute to the suppression of IFN-γ secretion. a HCV E1, E2, Core, NS3, NS4B, NS5A, and NS5B expression plasmids were used to transfect into primary CD4⁺ lymphocytes by Nucleofector. The frequencies of IFN-γ-secreting cells among the samples' CD4⁺ cells/the frequencies of IFN-γ-secreting cells among the vector's CD4⁺ cells ×100 are shown in this bar graph. b HCV core and NS5A transfected primary CD4⁺ lymphocytes were stimulated with IFN-γ (500 ng/ml). The relative expression of T-bet-mRNA was sequentially analyzed by real-time polymerase chain reaction (PCR). The relative amount of target mRNA was obtained by using a comparative the threshold cycle (CT) method. The expression level of mRNAs of the nonstimulation sample of vector transfected-primary CD4⁺ cells is represented as 1.0 and the relative amount of target mRNA in a stimulated sample was calculated. Three independent experiments were carried out. Error bars indicate the standard deviation. c Immunoblotting assay was carried out to detect the protein of signal transducer and activator of transcription-1 (STAT-1), phospho-STAT-1 (p-STAT-1), and actin in the HCV-core, NS5A, and vector-plasmid transfected human primary CD4⁺ cells with or without IFN-γ stimulation (30 min)

SB-HCV infection could induce apoptosis of naïve CD4⁺ cells

Annexin V and PI double staining were carried out to detect early apoptotic cells. The frequency of Annexin-V-positive PI-negative early apoptotic cells in SB-HCV-infected naïve T cells was significantly higher than those in the control groups ($p < 0.01$) (Fig. 3a, b). UV-irradiated SB-HCV did not enhance the induction of apoptosis in naïve T cells with CD3CD28 stimulation. During T-cell activation, apoptosis is easily induced in order to maintain an appropriate immune response. In line with this feature, 3.04% of early apoptotic cells were detected in naïve T cells with CD3CD28 beads stimulation and Mock serum. These data indicate that SB-HCV replication could induce apoptosis, as seen in Molt-4 cells [14].

HCV core and NS5A proteins could suppress IFN-γ secretion from primary CD4⁺ cells

We investigated the HCV proteins responsible for the suppression of IFN-γ secretion. HCV E1, E2, Core, NS3, NS4B, NS5A, and NS5B expression plasmids were used to transfect into primary CD4⁺ lymphocytes by Nucleofector. The intracellular staining of these proteins was carried out and the transfection efficiency was about 35–55% (Suppl. Fig. 3). Among these proteins, HCV core and NS5A could significantly suppress the IFN-γ secretion ($p < 0.05$) (Fig. 4). HCV core and NS5A transfected primary CD4⁺ lymphocytes were stimulated with IFN-γ. The relative expression of T-bet-mRNA was sequentially analyzed by real-time PCR. T-bet-mRNA expression in HCV core or NS5A transfected primary CD4⁺ T lymphocytes was significantly suppressed at 90 and 180 min post-transfection in comparison to vector-transfected primary CD4⁺ T lymphocytes. Moreover, the amount of STAT-1 protein in HCV-Core-expressing CD4⁺ cells was remarkably lower than the amounts in vector and HCV-E2 transfected CD4⁺ cells

Table 1 Cytokine conditions for various kinds of lymphoid cell culture

Cells	Cytokine condition	Other stimulant	Cell viability (%)
PBMC	IL2 (50 ng/ml) + IL6 (20 ng/ml) + CSF (250 ng/ml)	None	80
PBMC-CD8	IL2 (50 ng/ml) + IL6 (20 ng/ml) + CSF (250 ng/ml)	None	80
CD3	IL2 (50 ng/ml)	CD3CD28 coated beads	70
CD4	IL2 (50 ng/ml)	CD3CD28 coated beads	70
CD8	IL2 (50 ng/ml)	CD3CD28 coated beads	70
CD14	CSF (250 ng/ml)	None	60
CD19	IL-6 (20 ng/ml)	None	70

The conditions of the cell culture are shown. Peripheral blood mononuclear cell (PBMC)-CD8 indicates CD8 cell-depleted PBMCs

IL interleukin, CSF colony stimulating factor

Springer

Table 2 Strand-specific hepatitis C virus (HCV)-RNA detection in various kinds of lymphoid cells

Subset	PBMC	PBMC-CD8	CD3	CD4	CD8	CD14	CD19
Positive strand							
2 days	+	+	−	+	−	−	+
7 days	++	++	+	++	−	++	+++
7 days UV-irradiated	−	−	−	−	−	−	−
Negative strand							
2 days	−	−	−	−	−	−	−
7 days	−	+	+/−	+	−	+	++
7 days UV-irradiated	−	−	−	−	−	−	−

Subset	Whole CD4$^+$	CD4$^+$CD45RA$^+$RO$^-$	CD4$^+$CD45RA$^-$RO$^+$
Positive strand			
2 days	+	+	+
7 days	++	+++	+
7 days UV-irradiated	−	−	−
Negative strand			
2 days	−	−	−
7 days	+	++	+/−
7 days UV-irradiated	−	−	−

Positive- and negative-strand-specific HCV-RNA was detected by semiquantitative nested polymerase chain reaction (PCR) methods

−, negative detection; +, positive detection without dilution; ++, positive detection with 4 times dilution; +++, positive detection with 16 times dilution; ±, only one detection in three independent experiments. Three independent experiments were carried out. Similar results were obtained three times

(Fig. 4c). The amount of phosphorylated STAT-1 (p-STAT-1) after IFN-γ stimulation was also analyzed. The amount of p-STAT-1 in HCV-Core and NS5A expressing CD4$^+$ cells was remarkably lower than that in the vector control.

Discussion

There are many reports about the existence of extrahepatic HCV replication that might contribute to immune dysfunction [13, 14, 23–25]. We have reported that a specific SB-HCV strain could replicate in B- and T-cell lines and affect various immune systems [13, 14, 25]. However, the results of these studies were not definitely conclusive, since the cell lines were inappropriate to investigate the development and commitment of the lymphocytes. In the present study, we demonstrated that the SB-HCV strain could replicate in primary CD19$^+$ B cells, CD4$^+$ T cells, and CD14$^+$ monocytes with cytokine stimulation. Among the CD4$^+$ T cells, CD4$^+$CD45RA$^+$RO$^-$ naïve CD4$^+$ cells were the most susceptible to SB-HCV infection. One of the speculated reasons to explain why naïve CD4$^+$ cells with stimulation were most susceptible to SB-HCV infection is that T cells might temporarily express various kinds of molecules which may contribute to the HCV infection during T-cell development. The infectivity of naïve CD4$^+$ T cells was not as high as that of Molt-4 cells. However,

significant suppression of cell development and IFN-γ secretion were seen in SB-HCV-infected naïve T cells with CD3, CD28, and IL2 stimulation. UV-irradiated-HCV that could not replicate in the cells suppressed the IFN-γ secretion slightly. These data indicate that not only the effect of HCV replication but also the direct binding effects of HCV structured proteins might contribute to the suppression of IFN-γ secretion. One report indicated that HCV-core protein could interact with the complement receptor gC1qR and upregulate suppressor of cytokine signaling-1 (SOCS-1), accompanied by downregulation of signal transducer and activator of transcription-1 (STAT-1) phosphorylation in T cells [7]. Another possible explanation of the discrepancies between HCV infectivity and suppression of proliferation and IFN-γ secretion might be the low sensitivity of HCV antigen-immunostaining, since lower sensitivity of immunostaining in comparison to the nested PCR method was found in our previous study [13].

HCV-Core and -NS5A proteins were the proteins responsible for the suppression of IFN-γ secretion from T cells. Lin et al. [26] have documented that HCV-core protein causes the degradation of STAT-1 protein and suppresses the Jak-STAT pathway in hepatocytes. In our previous study, reduction of STAT-1 protein was detected in HCV-core transfected primary naïve T cells and HCV-replicating Molt-4 cells [13]. Moreover, inhibition of intrahepatic gamma interferon production by HCV-NS5A

in transgenic mice was recently reported [27]. Recently, detection of HCV replicative intermediate RNA in perihepatic lymph nodes was reported [28]. The disturbance of Th1 commitment might influence the development of HCV-specific CTL in perihepatic lymph nodes. The selective infection of certain T cells by HCV in vivo may explain why there is only relative HCV-specific T-cell suppression without general immune suppression.

Suppression of proliferation activity was seen in HCV-infected naïve T cells as well as HCV-infected Molt-4 cells [14]. The expression level of CD45RA, which is a surface marker of T-cell development, gradually declined along with cell proliferation. However, HCV-infected naïve T cells expressed significantly higher levels of CD45RA than the control groups. We previously reported that HCV replication could suppress Ras/MEK/ERK signaling of Molt-4 [14]. During T-cell development, T cells showed strong proliferation activity that might facilitate HCV replication in T cells. However, extensive proliferation of HCV in T cells might interfere with the proper development of T cells.

The induction of apoptosis was seen in SB-HCV-infected naive T lymphocytes with CD3CD28 and IL2 stimulation. It is known that, during T-cell activation from naïve to effector cells, T cells have to survive activation-induced cell death (AICD), which may contribute to the maintenance of an appropriate level of the immune response [29, 30]. However, some groups reported that HCV replication could inhibit apoptosis in hepatoma cell lines [31, 32]. The developmental stages and characteristics of naïve T cells might explain these contradictory results. During T-cell activation, apoptosis is easily induced in order to maintain an appropriate immune response.

In conclusion, HCV replication in human naïve T cells might affect their proliferation activity and Th1 development, as was shown in the cell lines used in a previous study. The results suggest that the infectivity of HCV in human naïve T lymphocytes is low, although the biological effect of this infection might be significant because of its bystander effects.

References

1. Alter MJ, Kruszon-Moran D, Nainan OV, McQuillan GM, Gao F, Moyer LA, et al. The prevalence of hepatitis C virus infection in the United States, 1988 through 1994. N Engl J Med. 1999; 341(8):556–62.

2. Chang KM, Rehermann B, Chisari FV. Immunopathology of hepatitis C. Springer Semin Immunopathol. 1997;19(1):57–68.

3. Ferri C, Caracciolo F, Zignego AL, La Civita L, Monti M, Longombardo G, et al. Hepatitis C virus infection in patients with non-Hodgkin's lymphoma. Br J Haematol. 1994;88(2):392–4.

4. Accapezzato D, Francavilla V, Paroli M, Casciaro M, Chircu LV, Cividini A, et al. Hepatic expansion of a virus-specific regulatory CD8(+) T cell population in chronic hepatitis C virus infection. J Clin Invest. 2004;113(7):963–72.

5. Manigold T, Racanelli V. T-cell regulation by CD4 regulatory T cells during hepatitis B and C virus infections: facts and controversies. Lancet Infect Dis. 2007;7(12):804–13.

6. Blackburn SD, Wherry EJ. IL-10, T cell exhaustion and viral persistence. Trends Microbiol. 2007;15(4):143–6.

7. Yao ZQ, Prayther D, Trabue C, Dong ZP, Moorman J. Differential regulation of SOCS-1 signalling in B and T lymphocytes by hepatitis C virus core protein. Immunology. 2008; 125(2):197–207.

8. Bare P, Massud I, Parodi C, Belmonte L, Garcia G, Nebel MC, et al. Continuous release of hepatitis C virus (HCV) by peripheral blood mononuclear cells and B-lymphoblastoid cell-line cultures derived from HCV-infected patients. J Gen Virol. 2005; 86(Pt 6):1717–27.

9. Hu Y, Shahidi A, Park S, Guilfoyle D, Hirshfield I. Detection of extrahepatic hepatitis C virus replication by a novel, highly sensitive, single-tube nested polymerase chain reaction. Am J Clin Pathol. 2003;119(1):95–100.

10. Laporte J, Bain C, Maurel P, Inchauspe G, Agut H, Cahour A. Differential distribution and internal translation efficiency of hepatitis C virus quasi species present in dendritic and liver cells. Blood. 2003;101(1):52–7.

11. Li Y, Wang X, Douglas SD, Metzger DS, Woody G, Zhang T, et al. CD8+ T cell depletion amplifies hepatitis C virus replication in peripheral blood mononuclear cells. J Infect Dis. 2005;192(6):1093–101.

12. Sung VM, Shimodaira S, Doughty AL, Picchio GR, Can H, Yen TS, et al. Establishment of B-cell lymphoma cell lines persistently infected with hepatitis C virus in vivo and in vitro: the apoptotic effects of virus infection. J Virol. 2003;77(3):2134–46.

13. Kondo Y, Sung VM, Machida K, Liu M, Lai MM. Hepatitis C virus infects T cells and affects interferon-gamma signaling in T cell lines. Virology. 2007;361(1):161–73.

14. Kondo Y, Machida K, Liu HM, Ueno Y, Kobayashi K, Wakita T, et al. Hepatitis C virus infection of T cells inhibits proliferation and enhances fas-mediated apoptosis by down-regulating the expression of CD44 splicing variant 6. J Infect Dis. 2009; 199(5):726–36.

15. Lindenbach BD, Evans MJ, Syder AJ, Wolk B, Tellinghuisen TL, Liu CC, et al. Complete replication of hepatitis C virus in cell culture. Science. 2005;309(5734):623–6.

16. Wakita T, Pietschmann T, Kato T, Date T, Miyamoto M, Zhao Z, et al. Production of infectious hepatitis C virus in tissue culture from a cloned viral genome. Nat Med. 2005;11(7):791–6.

17. Kato T, Date T, Murayama A, Morikawa K, Akazawa D, Wakita T. Cell culture and infection system for hepatitis C virus. Nat Protoc. 2006;1(5):2334–9.

18. Negro F, Krawczynski K, Quadri R, Rubbia-Brandt L, Mondelli M, Zarski JP, et al. Detection of genomic- and minus-strand of hepatitis C virus RNA in the liver of chronic hepatitis C patients by strand-specific semiquantitative reverse-transcriptase polymerase chain reaction. Hepatology. 1999;29(2):536–42.

19. Machida K, Cheng KT, Sung VM, Lee KJ, Levine AM, Lai MM. Hepatitis C virus infection activates the immunologic (type II) isoform of nitric oxide synthase and thereby enhances DNA

damage and mutations of cellular genes. J Virol. 2004;78(16): 8835–43.

20. Harris HJ, Farquhar MJ, Mee CJ, Davis C, Reynolds GM, Jennings A, et al. CD81 and claudin 1 coreceptor association: role in hepatitis C virus entry. J Virol. 2008;82(10):5007–20.

21. Molina S, Castet V, Pichard-Garcia L, Wychowski C, Meurs E, Pascussi JM, et al. Serum-derived hepatitis C virus infection of primary human hepatocytes is tetraspanin CD81 dependent. J Virol. 2008;82(1):569–74.

22. Cormier EG, Tsamis F, Kajumo F, Durso RJ, Gardner JP, Dragic T. CD81 is an entry coreceptor for hepatitis C virus. Proc Natl Acad Sci USA. 2004;101(19):7270–4.

23. Kanto T, Inoue M, Miyatake H, Sato A, Sakakibara M, Yakushijin T, et al. Reduced numbers and impaired ability of myeloid and plasmacytoid dendritic cells to polarize T helper cells in chronic hepatitis C virus infection. J Infect Dis. 2004; 190(11):1919–26.

24. Kanto T, Hayashi N, Takehara T, Tatsumi T, Kuzushita N, Ito A, et al. Impaired allostimulatory capacity of peripheral blood dendritic cells recovered from hepatitis C virus-infected individuals. J Immunol. 1999;162(9):5584–91.

25. Machida K, Kondo Y, Huang JY, Chen YC, Cheng KT, Keck Z, et al. Hepatitis C virus (HCV)-induced immunoglobulin hypermutation reduces the affinity and neutralizing activities of antibodies against HCV envelope protein. J Virol. 2008;82(13): 6711–20.

26. Lin W, Choe WH, Hiasa Y, Kamegaya Y, Blackard JT, Schmidt EV, et al. Hepatitis C virus expression suppresses interferon signaling by degrading STAT1. Gastroenterology. 2005;128(4): 1034–41.

27. Kanda T, Steele R, Ray R, Ray RB. Inhibition of intrahepatic gamma interferon production by hepatitis C virus nonstructural protein 5A in transgenic mice. J Virol. 2009;83(17):8463–9.

28. Pal S, Sullivan DG, Kim S, Lai KK, Kae J, Cotler SJ, et al. Productive replication of hepatitis C virus in perihepatic lymph nodes in vivo: implications of HCV lymphotropism. Gastroenterology. 2006;130(4):1107–16.

29. Krammer PH. CD95's deadly mission in the immune system. Nature. 2000;407(6805):789–95.

30. Holmstrom TH, Schmitz I, Soderstrom TS, Poukkula M, Johnson VL, Chow SC, et al. MAPK/ERK signaling in activated T cells inhibits CD95/Fas-mediated apoptosis downstream of DISC assembly. EMBO J. 2000;19(20):5418–28.

31. Nanda SK, Herion D, Liang TJ. The SH3 binding motif of HCV [corrected] NS5A protein interacts with Bin1 and is important for apoptosis and infectivity. Gastroenterology. 2006;130(3):794–809.

32. Miyasaka Y, Enomoto N, Kurosaki M, Sakamoto N, Kanazawa N, Kohashi T, et al. Hepatitis C virus nonstructural protein 5A inhibits tumor necrosis factor-alpha-mediated apoptosis in Huh7 cells. J Infect Dis. 2003;188(10):1537–44.

Hepatitis B Virus Replication Could Enhance Regulatory T Cell Activity by Producing Soluble Heat Shock Protein 60 From Hepatocytes

Yasuteru Kondo,[1] Yoshiyuki Ueno,[1] Koju Kobayashi,[2] Eiji Kakazu,[1] Masaaki Shiina,[1] Jun Inoue,[1] Keiichi Tamai,[1] Yuta Wakui,[1] Yasuhito Tanaka,[5] Masashi Ninomiya,[1] Noriyuki Obara,[1] Koji Fukushima,[1] Motoyasu Ishii,[3] Tomoo Kobayashi,[4] Hirofumi Niitsuma,[1] Satonori Kon,[2] and Tooru Shimosegawa[1]

[1]Division of Gastroenterology, Tohoku University Hospital, [2]School of Health Science, Tohoku University, [3]Department of Gastroenterology, Miyagi Social Insurance Hospital, and [4]Department of Gastroenterology, Tohoku Rosai Hospital, Sendai, and [5]Clinical Molecular Informative Medicine, Nagoya City University, Nagoya, Japan

Background. HBcAg-specific regulatory T (T_{reg}) cells play an important role in the pathogenesis of chronic hepatitis B. Soluble heat shock proteins, especially soluble heat shock protein 60 (sHSP60), could affect the function of T_{reg} cells via Toll-like receptor.

Methods. We analyzed the relationship between soluble heat shock protein production and hepatitis B virus (HBV) replication with both clinical samples from HBeAg-positive patients with chronic hepatitis B ($n = 24$) and HBeAb-positive patients with chronic hepatitis B ($n = 24$) and in vitro HBV-replicating hepatocytes. Thereafter, we examined the biological effects of sHSP60 with isolated T_{reg} cells.

Results. The serum levels of sHSP60 in patients with chronic hepatitis B were statistically significantly higher than those in patients with chronic hepatitis C ($P < .01$), and the levels of sHSP60 were correlated with the HBV DNA levels ($R = 0.532$; $P < .001$) but not with the alanine aminotransferase levels. Moreover, the levels of sHSP60 in HBV-replicating HepG2 cells were statistically significantly higher than those in control HepG2 cells. Preincubation of CD4$^+$ CD25$^+$ cells with recombinant HSP60 (1 ng/mL) statistically significantly increased the frequency of HBcAg-specific interleukin 10–secreting T_{reg} cells. The frequency of IL7R$^-$CD4$^+$CD25$^+$ cells, the expression of Toll-like receptor 2, and the suppressive function of T_{reg} cells had declined during entecavir treatment.

Conclusion. The function of HBcAg-specific T_{reg} cells was enhanced by sHSP60 produced from HBV-infected hepatocytes. Entecavir treatment suppressed the frequency and function of T_{reg} cells; this might contribute to the persistence of HBV infection.

Hepatitis B virus (HBV) is a noncytopathic DNA virus that causes chronic hepatitis and hepatocellular carcinoma as well as acute hepatitis and fulminant hepatitis [1]. HBV now affects more than 400 million people worldwide [2], and persistent infection develops in

~5% of adults and 95% of neonates who become infected with HBV.

It has been shown that the cellular immune system, including cytotoxic T lymphocytes, CD4$^+$ T helper 1 cells, and CD4$^+$C25$^+$FoxP3$^+$ regulatory T (T_{reg}) cells, plays a central role in the control of viral infection [3–6]. The hyporesponsiveness of HBV-specific T helper 1 cells and the excessive regulatory function of T_{reg} cells in peripheral blood in patients with chronic hepatitis B has been shown elsewhere [7–10]. Lamivudine treatment of chronic hepatitis B has been reported to restore both CD4$^+$ T cells and cytotoxic T lymphocyte hyporesponsiveness following the decrease of serum levels of HBV DNA and HBV-derived Ag [8, 11–13]. In our previous study, we observed that HBcAg-specific interleukin 10 (IL-10)–secreting T_{reg} cells could play an important role in the immunopathogenesis of chronic hepatitis B [9].

Table 1. Clinical Characteristics of Patients with Chronic Hepatitis B or Chronic Hepatitis C Included in This Study

Characteristic	Patients with chronic hepatitis B		Patients with chronic hepatitis C
	HBeAg-positive, HBeAb-negative patients	HBeAg-negative, HBeAb-positive patients	
Age, years	45.16 (12.46)	48.21 (10.23)	48.63 (7.96)
Sex, no. of patients			
Male	12	12	12
Female	12	12	12
ALT level, IU/L	76.91 (39.82)	75.96 (45.90)	76.21 (33.77)
HBV DNA level, log copies/mL	7.83 (0.86)	6.00 (0.81)	NA
Genotype, % of patients			
A	0	4.17	NA
B	12.5	8.33	NA
C	87.5	87.5	NA

NOTE. Data are mean values (standard deviations), unless otherwise indicated. ALT, alanine aminotransferase; HBV, hepatitis B virus; NA, not applicable.

Many research groups have reported the possible induction of anergy by T_{reg} cells, which constitutively express CD25 (the interleukin 2 receptor α chain) in the physiological state [14–16]. In humans, this population of T_{reg} cells, as defined by $CD4^+CD25^+CTLA4^+$ cells, $CD4^+CD25^+FoxP3^+$ cells, or $CD4^+CD25^+IL7R^-$ cells, constitutes 5%–10% of peripheral $CD4^+$ T cells and has a broad repertoire that recognizes various self and nonself antigens. It has been reported that T_{reg} cells have several different mechanisms in suppressing various kinds of immune cells [17, 18]. The important mechanisms are cell to cell contact and secretion of cytokines including IL-10 and transforming growth factor β (TGF-β) [19, 20]. HBcAg derived from HBV might induce T_{reg} cells to escape from immunological pressure, as reported in persistent infection with Epstein-Barr virus, hepatitis C virus (HCV), and human immunodeficiency virus type 1 [21–23]. Some results have indicated that reduction of HBV replication could reduce the frequency and/or function of T_{reg} cells in patients with chronic hepatitis B [4, 5, 8]. However, the key factors that affect HBcAg-specific T_{reg} cells in the replication of HBV remain unclear.

The mammalian 60-kDa heat shock protein is a many-faceted molecule. In addition to serving as a chaperone, heat shock protein 60 (HSP60) is expressed by different types of cells following their exposure to stress or immune responses and is present in the blood during inflammation [24–27]. Recently, HSP60 was reported to enhance the function of $CD4^+CD25^+$ regulatory T cell function via Toll-like receptor 2 (TLR2) signaling [28].

In this study, we investigated the serum level of HSP60 in patients with chronic hepatitis B and the relevance of HBcAg-specific IL-10-secreting T_{reg} cells and HSP60. We report evidence of the production of soluble HSP60 (sHSP60) from HBV-replicating hepatocytes, by use of clinical samples from patients

with chronic hepatitis B and an in vitro HBV replication system. In addition, reductions of $CD4^+CD25^+IL7R^-$ T_{reg} cells and TLR2 expression on T_{reg} cells were observed during entecavir therapy. This study could contribute to better understanding of the immunopathogenesis of chronic hepatitis B and the development of immune-based treatment.

MATERIALS AND METHODS

Patients. Forty-eight patients with chronic hepatitis B were enrolled in this study (Table 1). The patients had serum levels of HBV DNA of >5.0 log copies/mL and had elevated alanine aminotransferase (ALT) levels (reference range, <40 IU/L) for >6 months prior to the study. To focus the analysis on the active phase of chronic hepatitis B, we excluded asymptomatic carriers and patients with immune tolerance by age (<30 years old), ALT values (<40 IU/L), and HBV DNA levels (<5.0 log copies/mL). Twenty-four patients were seropositive for HBeAg, and 24 patients were seropositive for anti-HBeAb. None of the patients tested positive for antibodies to hepatitis C virus or had liver disease due to other causes, such as alcohol, drugs, congestive heart failure, and autoimmune disease. Twenty-four patients with chronic hepatitis C and 10 healthy subjects were included as control subjects. Permission for the study was obtained from the Ethics Committee at Tohoku University Graduate School of Medicine (permission no. 2006-194]). Written informed consent was obtained from all the participants enrolled in this study. Participants were monitored for 6 months, and peripheral blood samples were obtained and assessed at 1, 2, 3, and 6 months. At each assessment, patients were evaluated for serum levels of HBV DNA, HBeAg, and anti-HBe, blood chemistry, and hematology. Levels of HBsAg, anti-HBs, total and immunoglobulin anti-HBc, HBeAg, anti-HBe, and anti–

hepatitis C virus were determined by means of commercial enzyme immunoassay kits (Abbott Laboratories). Serum levels of HBV DNA were measured by means of an Amplicor polymerase chain reaction (PCR) assay (lower limit of detection, 2.6 log copies/mL; Roche). High titers of HBV DNA were measured by means of a transcription-mediated amplification-hybridization protection assay (TMA; lower limit of detection, 3.7 log genome equivalents per milliliter). Data were adjusted by means of the following formula: Amplicor value = 0.83 × (TMA value) + 0.67.

Reagents. The following antibodies were used: CD3–allophycocyanin (APC), CD4–peridinin chlorophyll protein complex (PerCP), CD25–fluorescein isothiocyanate (FITC), CD25-phycoerythrin (PE), CD127-PE, Alexa Fluor 488 mouse anti–human CD282 (TLR2), CD284 (Toll-like receptor 4 [TLR4]), and isotype-matched control antibodies purchased from BD Bioscience. Recombinant HBcAg was obtained from Biodesign International. Recombinant HSP60 (rHSP60) was purchased from Stressgen.

Quantification of sHSP60 and soluble heat shock protein 70 (sHSP70) levels. Levels of HSP60 and heat shock protein 70 (HSP70) were quantified by use of HSP60 and HSP70 enzyme-linked immunosorbent assay (ELISA) kits (Stressgen). The serum samples from patients and supernatants from cell cultures were collected at sampling points and stocked at −20°C. The ELISA procedure was performed according to the manufacturer's protocol. First, 100-μL prepared samples were added to wells of anti-HSP60-coated plates. Then the reaction of the anti-HSP60 and horseradish peroxidase conjugate was performed after incubation and washing. Absorbance was measured at 450 nm. The HSP60 sample concentration was calculated by use of a standard curve.

Isolation of peripheral blood mononuclear cells (PBMCs) and T_{reg} cells. PBMCs were isolated from fresh heparinized blood by means of Ficoll-Hypaque density gradient centrifugation. T_{reg} cells were isolated by use of a Dynabeads regulatory $CD4^+CD25^+$ T cell kit (Invitrogen). T_{reg} cells were isolated according to the manufacturer's protocol. In brief, $CD4^+$ cells were isolated from PBMCs by means of negative selection. The remaining cells included the PBMCs depleted of $CD4^+$ cells. Then the $CD4^+CD25^+$ cells were selected positively by use of $CD25^+$ antibody combined with beads. Finally, the beads were detached by means of Detachabead (Invitrogen), because the function of T_{reg} cells might be modified by anti-CD25 antibody.

Coculture of γ-irradiated HBcAg-presenting antigen-presenting cells (APCs) and T_{reg} cells. During the isolation of T_{reg} cells, PBMCs depleted of $CD4^+$ cells could be obtained for use as APCs. PBMCs depleted of $CD4^+$ cells were stimulated at 1×10^6 cells/mL in Roswell Park Memorial Institute 1640 medium containing 10% fetal bovine serum with HBcAg (10 μg/mL) for 12 h at 37°C. Then these γ-irradiated cells were

coincubated with 1×10^5 isolated T_{reg} cells that were untreated pretreated with TLR2 and TLR4 neutralizing antibody and rHSP60 (1 ng/mL) (Figures 1A and 2).

IL-10 secretion assay. Isolated T_{reg} cells were stimulated with HBcAg-presenting autologous γ-irradiated APCs for 12 h at 37°C. IL-10-secreting cells were stained by adding 10 μL of IL-10-detection antibody (PE-conjugated) together with anti-CD4-PerCP, anti-CD25-FITC, and anti-CD3-APC.

Flow cytometry. PBMCs were stained with CD3-APC, CD4-PerCP, CD25-FITC, and CD127-PE antibodies for 15 min on ice to analyze the frequency of $CD4^+CD25^+IL7R^-$ cells. CD4-PerCP, CD25-PE, and Alexa Fluor 488 mouse anti–human CD282 (TLR2) or CD284 (TLR4) were used for the analysis of TLR2 and TLR4 expression on $CD4^+CD25^+$ cells. Isotype-matched control antibodies were used for adjustment of the fluorescence intensity.

Construction of plasmids. The HBV plasmids was constructed as described elsewhere, with minor modifications [29]. In brief, a serum sample from one of the consecutive patients with fulminant hepatitis B (fulminant hepatitis clone 2), whose serum level of HBV DNA was the highest of the 5 patients, was used to extract total DNA (QIAamp DNA blood mini kit; Qiagen), which was subjected to nested PCR for 2 overlapping fragments; the amplified fragments were nucleotides 1051–3215/1–327 (2492 nucleotides; fragment A) and nucleotides 180–1953 (1774 nucleotides; fragment B). Then the vectors were digested with XbaI, and the XbaI-XbaI site of fragment A-pUC118 was ligated to the XbaI-XbaI site of fragment B-pUC118. Finally, a plasmid containing a 1.3-fold HBV genome (nucleotides 1051–3215/1–1953) was constructed and named pBFH2.

Cell culture and transfection. Human hepatoma HepG2 cells were incubated in Dulbecco modified Eagle medium supplemented with 10% bovine serum at 37°C and 5% carbon dioxide. For the assay of HBV replication, 6-well plates were seeded with 5×10^5 HepG2 or Huh7 cells each. On the next day, 1.5 μg of plasmid DNA were transfected to these cells by use of TransIT LT-1 transfection reagent (Mirus), and the culture supernatant and cells were collected 3 d later. The transfection efficiency was evaluated with a Great EscAPe secreted alkaline phosphatase reporter system 3 (Clontech), in which 10 ng/mL of a reporter plasmid expressing secreted alkaline phosphatase was cotransfected. Experiments were performed at least in triplicate.

Quantification of extracellular HBV DNA, HBsAg, and HBeAg levels. To digest the input plasmid DNA in the culture supernatant, 5 μL of the supernatant was treated with 5 U of DNase I (TaKaRa Bio) at 37°C for 1 h, and the reaction was stopped with edetic acid. Then total DNA was extracted with a QIAamp DNA blood mini kit, and 10 μL of 200-μL DNA solution was subjected to real-time PCR by use of a LightCycler
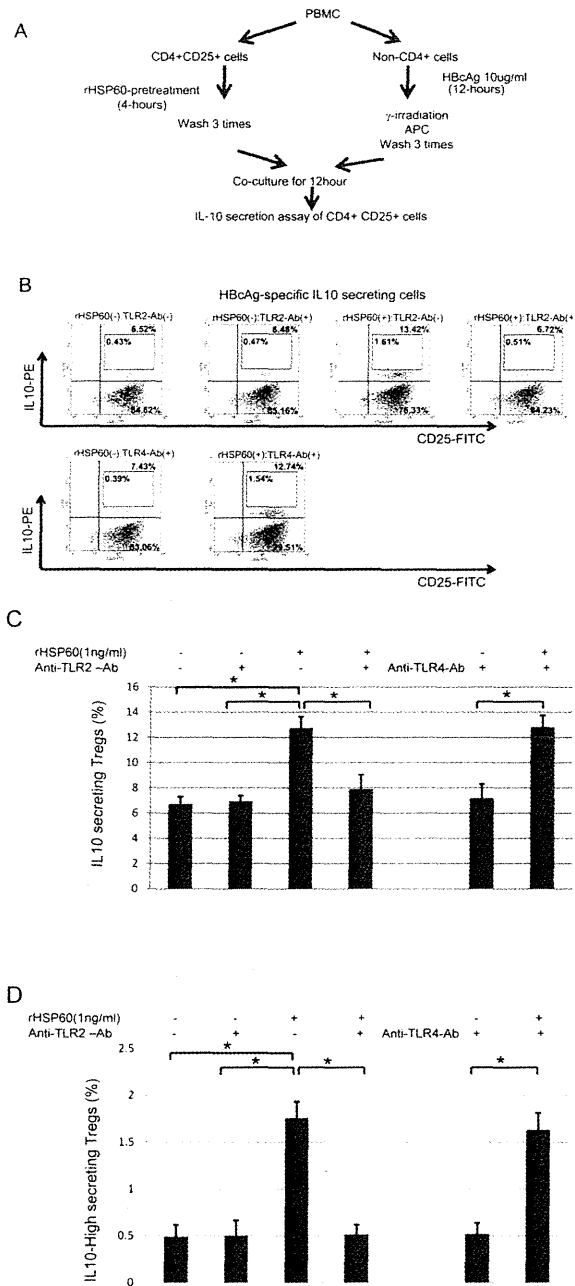
A

PBMC

CD4+CD25+ cells   Non-CD4+ cells

rHSP60-pretreatment   HBcAg 10ug/ml
(4-hours)   (12-hours)

Wash 3 times   γ-irradiation
                                 APC
                                 Wash 3 times

Co-culture for 12hour

IL-10 secretion assay of CD4+ CD25+ cells

B

HBcAg-specific IL10 secreting cells

rHSP60(-):TLR2-Ab(-)   rHSP60(-):TLR2-Ab(+)   rHSP60(+):TLR2-Ab(-)   rHSP60(+):TLR2-Ab(+)
6.52%   6.48%   13.42%   6.72%
0.43%   0.47%   1.61%   0.51%
84.82%   83.16%   78.33%   84.23%

IL10-PE   CD25-FITC

rHSP60(-):TLR4-Ab(+)   rHSP60(+):TLR4-Ab(+)
7.43%   12.74%
0.39%   1.54%
83.06%   75.51%

IL10-PE   CD25-FITC

C

rHSP60(1ng/ml)   -   -   +   +   -   +
Anti-TLR2 –Ab   -   +   -   + Anti-TLR4-Ab +   +

IL10 secreting Tregs (%)

D

rHSP60(1ng/ml)   -   -   +   +   -   +
Anti-TLR2 –Ab   -   +   -   + Anti-TLR4-Ab +   +

IL10-High secreting Tregs (%)

Figure 1. Effects of heat shock protein 60 (HSP60) on HBcAg-specific interleukin 10 (IL-10)–secreting regulatory T (T_{reg}) cells. A, Flow chart of the methods. B, Representative dot plots of IL-10-secreting cells in the CD4+CD25+ cells. The mixed cells (antigen-presenting cells [APCs; CD4−] and isolated CD4+CD25+ cells) were stained with anti-CD4–peridinin chlorophyll protein complex (PerCP), anti-CD25–fluorescein isothiocyanate (FITC), and anti-IL-10-phycoerythrin (PE). The numbers in each top right quadrant indicate the frequencies of CD25+ IL-10-secreting cells among the CD4+ cells. The numbers in each bottom right quadrant indicate the frequencies of CD4+CD25+IL-10− cells among the CD4+ cells. The numbers in each box in the top right quadrant indicate the frequencies of CD25+ IL-10-secreting cells among the CD4+ cells. C, Representative results for a sample from 1 patient with chronic hepatitis B (samples were obtained from 3 patients with chronic hepatitis B; this experiment was repeated 3 times). Bars indicate the percentage of IL-10-secreting cells among the CD4+ cells with various kinds of pretreatment. D, Percentage of high–IL-10-secreting cells among the CD4+ cells. Error bars indicate the standard deviation of 3 independent experiments with a sample from 1 patient with chronic hepatitis B. Three independent experiments yielded similar results to those shown in panels C and D. *$P < .05$.

Figure 2. Effect of recombinant heat shock protein 60 (rHSP60) on the interleukin 10 (IL-10)–secreting activity of CD4⁺CD25⁺ cells.

system (Roche). ELISA kits were used to assay HBsAg (Hope Laboratories) and HBeAg (BioChain Institute) in 50 μL of the culture supernatant.

Sequence analysis of HBV DNA. The presence of HBV DNA in the serum samples was determined by means of PCR, as described elsewhere [30]. Nucleic acids were extracted from 100 mL of serum and subjected to nested PCR for the S gene. The amplification product of the first-round PCR was 461 bp, and that of the second-round PCR was 437 bp. The amplification products were sequenced directly on both strands by use of the BigDye Terminator Cycle Sequencing Ready reaction kit on an ABI Prism 3100 genetic analyzer (Applied Biosystems).

Carboxyfluorescein succinimidyl ester (CFSE) staining and suppression assay. The suppressive activity of regulatory T cells was analyzed by use of a CellTrace CFSE cell proliferation kit (Molecular Probes). Staining methods were followed according to the manufacturer's protocol. Briefly, the collected CD4⁺CD25⁻ cells were washed and resuspended in prewarmed phosphate-buffered saline with 0.1% bovine serum albumin at a final concentration of 3×10^5 cells/mL. CFSE solution (5 μm) was added and incubated at 37°C for 10 min. Stained cells were washed 3 times and incubated with unstained CD4⁺CD25⁺ T_{reg} cells and CD3CD28-coated stimulation beads (T cell expander) for an additional 3 d. The cells were analyzed by means flow cytometry with 488-nm excitation and emission filters.

Statistics. The data in Figures 3, 4, 1C, 1D, and 5 were analyzed by use of the independent t test. Statistical correlation analysis of the data in Figure 6 was performed by use of the Kendall τ_b test. The data in Figure 7 were analyzed by use of the Wilcoxon rank sum test. All of the statistical analyses were performed with SPSS software (version 10.0; SPSS). Results for which $P < .05$ were considered to be statistically significant.

RESULTS

Levels of sHSP60 and sHSP70 in samples from HBeAg-positive patients with chronic hepatitis B, HBeAg-negative patients with chronic hepatitis B, and control patients with chronic hepatitis C. The patients' characteristics, including age, sex, and ALT level, were matched among the different patient groups because the levels of sHSP60 and sHSP70 might be influenced by these factors (Table 1). The mean ($\pm$ standard deviation [SD]) serum level of sHSP60 was 5.77 $\pm$ 1.19 ng/mL in HBeAg-positive patients with chronic hepatitis B, 4.12 $\pm$ 1.37 ng/mL in HBeAg-negative patients with chronic hepatitis B, 2.11 $\pm$

0.96 ng/mL in patients with chronic hepatitis C, and 0.54 $\pm$ 0.46 ng/mL in healthy subjects. The levels of sHSP60 in patients with chronic hepatitis B (HBeAg-positive and HBeAg-negative) were statistically significantly higher than those in patients with chronic hepatitis C (Figure 3). On the other hand, the mean ($\pm$ SD) serum level of sHSP70 was 7.89 $\pm$ 3.51 ng/mL in HBeAg-positive patients with chronic hepatitis B, 7.73 $\pm$ 3.71 ng/mL in HBeAg-negative patients with chronic hepatitis B, 8.09 $\pm$ 3.64 ng/mL in patients with chronic hepatitis C, and 3.54 $\pm$ 0.46 ng/mL in healthy subjects. There were no statistically significant differences in the level of sHSP70 between the chronic hepatitis B and chronic hepatitis C patient groups (Figure 3). Then we examined the correlations between the HSP60, HSP70, and HBV DNA or ALT levels. The levels of sHSP60 were correlated with the HBV DNA levels ($r = 0.532$; $P < .001$) but not with the ALT levels ($r = 0.101$; $P = .315$) (Figures 6A and 6B). On the other hand, the levels of sHSP70 were correlated with the ALT levels ($r = 0.520$; $P < .001$) but not with the HBV DNA levels ($r = 0.076$; $P < .449$) (Figure 6C and 6D).

HBV replication could directly induce sHSP60 production in vitro. Two kinds of plasmids carrying a 1.3-fold HBV genome that could replicate in HepG2 cells were used to analyze whether HBV replication could affect the production of sHSP60 in culture medium. The transfection efficiency was almost the
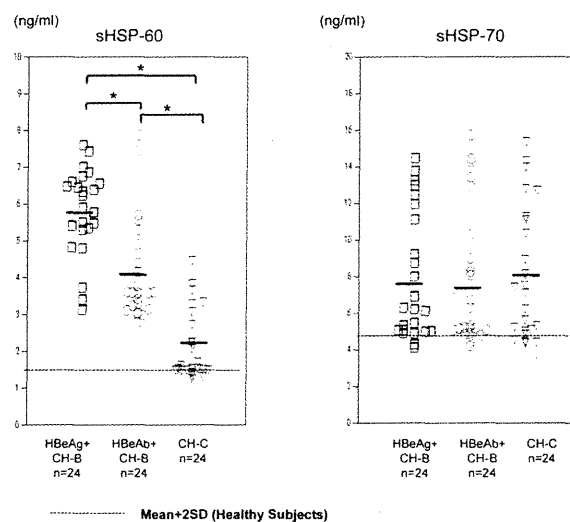

Figure 3. Quantification of serum levels of heat shock protein 60 (HSP60) and heat shock protein 70 (HSP70) in HBeAg-positive patients with chronic hepatitis B (CH-B), HBeAb-positive patients with CH-B, and patients with chronic hepatitis C (CH-C). Serum levels of HSP60 and HSP70 were quantified by means of enzyme-linked immunosorbent assay. The bar represents the means of the levels of HSP60 and HSP70. Dotted lines indicate the mean value plus 2 times the standard deviation (SD) of the levels of healthy subjects.
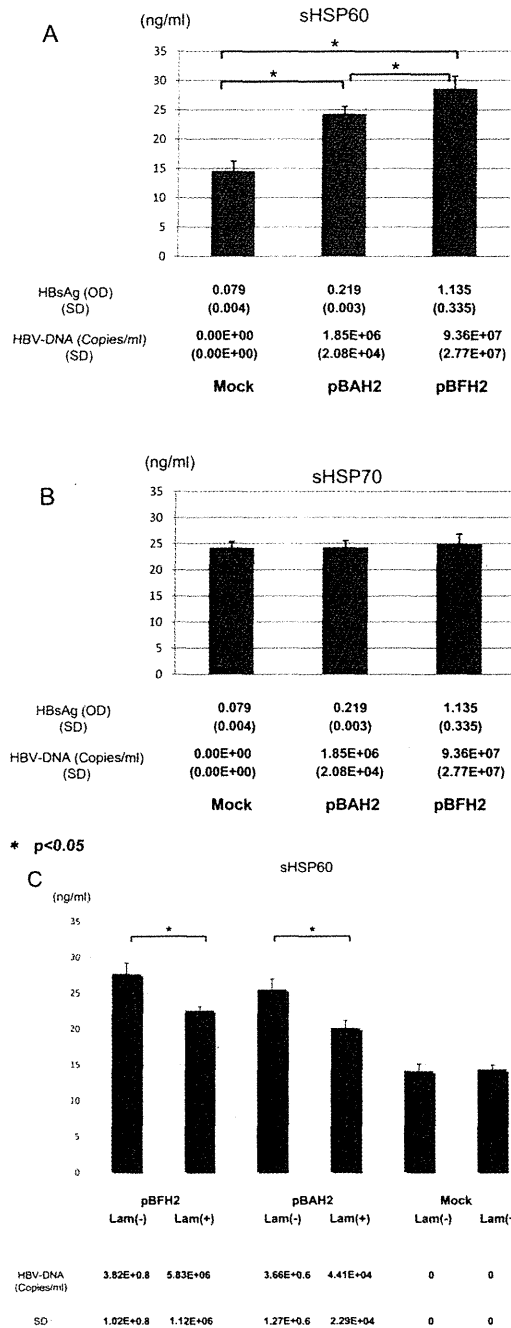
Figure 4. Direct effect of hepatitis B virus (HBV) on the production of heat shock protein 60 (HSP60) and heat shock protein 70 (HSP70). Two kinds of plasmid (pBAH2 and pBFH2) carrying a 1.3-fold HBV genome that could replicate in HepG2 cells and a mock plasmid were used to analyze whether HBV replication affects the production of soluble HSP60 (sHSP60) in culture medium. The levels of sHSP60 and soluble HSP70 (sHSP70) were compared among the 3 plasmid groups. Bars indicate the levels of HSP60 (A) and HSP70 (B). The HBsAg and HBV DNA levels and standard deviations (SDs) are included below the bar graphs. C, Levels of sHSP60 in cells with and those in cells without lamivudine treatment. The cells were treated with lamivudine (Lam; 0.5 μmol/L) for 72 h. Three independent experiments were performed.
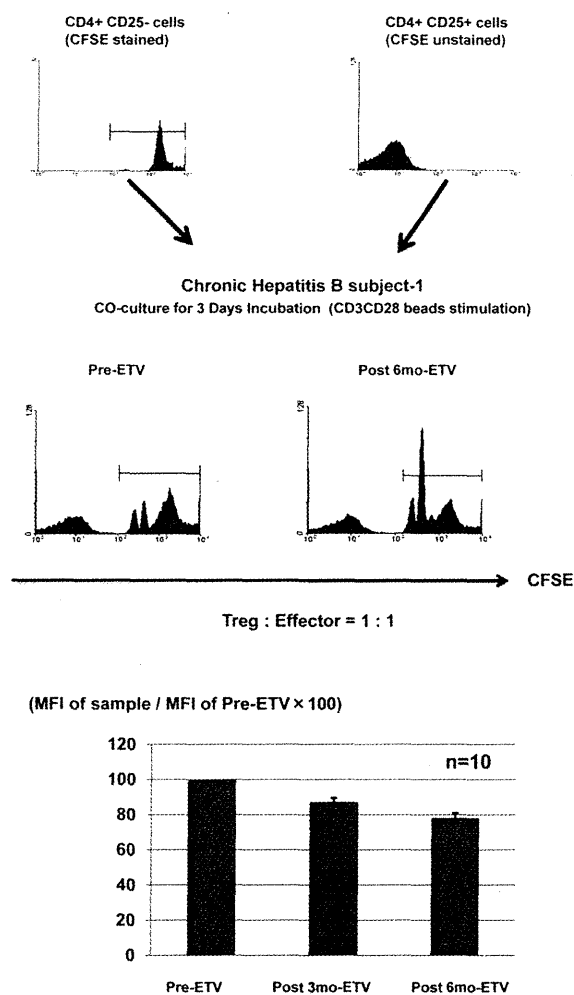
CD4+ CD25- cells
(CFSE stained)

CD4+ CD25+ cells
(CFSE unstained)

Chronic Hepatitis B subject-1
CO-culture for 3 Days Incubation (CD3CD28 beads stimulation)

Pre-ETV   Post 6mo-ETV

→ CFSE

Treg : Effector = 1 : 1

(MFI of sample / MFI of Pre-ETV × 100)

n=10

Pre-ETV   Post 3mo-ETV   Post 6mo-ETV

Figure 5. Suppression assay of regulatory T (T_{reg}) cells. The suppressive activity of T_{reg} cells was analyzed by means of coincubation of unstained isolated T_{reg} cells and autologous CD4⁺CD25⁻ cells with carboxyfluorescein succinimidyl ester (CFSE) staining. A, Representative histogram of CFSE-stained CD4⁺CD25⁻ effector cells and unstained CD4⁺CD25⁺ T_{reg} cells. B, Various levels of cell division in CD4⁺CD25⁻ effector cells observed 3 d after coincubation with CD3CD28-coated beads. C, Mean fluorescence intensity (MFI) of CFSE staining of CD4⁺CD25⁻ cells before treatment, 3 months after the start of entecavir (ETV) treatment, and 6 months after the start of entecavir treatment. The bars show the MFI of the samples divided by the MFI of the pretreatment samples ×100. The error bars indicate the standard deviations of the data.

same among the different plasmids (data not shown). The mean (± SD) HBV DNA levels of pBAH2 and pBFH2 were $1.85 \times 10^6 \pm 2.08 \times 10^4$ and $9.36 \times 10^7 \pm 2.77 \times 10^7$ copies/mL, respectively. The levels of sHSP60 in the supernatant of the pBAH2- and pBFH2-transfected HepG2 cells were statistically significantly higher than that of the mock-transfected HepG2 cells ($P < .05$) (Figure 4A). However, the levels of

sHSP70 in the supernatant of the pBAH2- and pBFH2-transfected HepG2 cells were comparable with that of the mock-transfected HepG2 cells (Figure 4B). The addition of HBV-derived antigen in the culture supernatant could not increase the level of sHSP60 (data not shown). We performed the experiment on the suppression of HBV replication by nucleoside analogues in vitro. The suppression of HBV replication could statistically significantly reduce the production of sHSP60 (Figure 4C). These data indicate that HBV replication could increase the level of sHSP60 in the supernatant of the hepatocyte culture.

The effect of HSP60 on the HBcAg-specific IL-10-secreting T_{reg} cells. Previously, we found that HBcAg-specific IL-10-secreting cells could play an important role in the hyporesponsiveness of T cells in patients with chronic hepatitis B [9]. The effects of HSP60 on HBcAg-specific IL-10-secreting T_{reg} cells were analyzed. The appropriate dose of rHSP60 pretreatment was determined by use of PBMCs from healthy subjects (Figure 2). Pretreatment with rHSP60 could increase the frequency of HBcAg-specific IL-10-secreting cells statistically significantly ($P < .01$) and enhance the function of IL-10 secretion of HBcAg-specific T_{reg} cells, because the frequencies of high-intensity cells with IL-10 staining in HSP60 pretreatment T_{reg} cells were statistically significantly higher than those of control groups (Figure 1D). Moreover, these effects were completely blocked by neutralizing TLR2 antibody but not by TLR4 antibody. These data indicate that HSP60 might enhance the susceptibility and function of IL-10 secretion of HBcAg-specific T_{reg} cells.

Sequential analysis of clinical samples collected during entecavir therapy. Ten patients were selected for sequential analysis during entecavir therapy. The titers of HBV DNA and the ALT level rapidly decreased during entecavir therapy (Figures 7A and 7B). The serum levels of HSP60 had statistically significantly decreased at 3 months and at 6 months after the start of entecavir therapy. The frequency of T_{reg} cells and the expression level of TLR2 during entecavir treatment were quantified sequentially for up to 6 months during treatment by means of flow cytometry analysis. The frequency of CD4⁺CD25⁺ cells decreased, although not statistically significantly. On the other hand, the frequency of CD4⁺CD25⁺IL7R⁻ cells (subpopulation of CD4⁺CD25⁺ cells) had statistically significantly decreased at 3 months and at 6 months after the start of entecavir therapy. The reason for the discrepancy could be that CD4⁺CD25⁺ cells included not only T_{reg} cells but also activated CD4⁺ effector cells. Previously, some research groups had found that CD4⁺CD25⁺FoxP3⁺ cells are almost the same as CD4⁺CD25⁺IL7R⁻ cells. Therefore, our data indicate that entecavir therapy could reduce the frequency of T_{reg} cells. We also investigated the frequency of CD4⁺CD25⁺FoxP3⁺ cells during lamivudine therapy (Figure 8). The frequency of
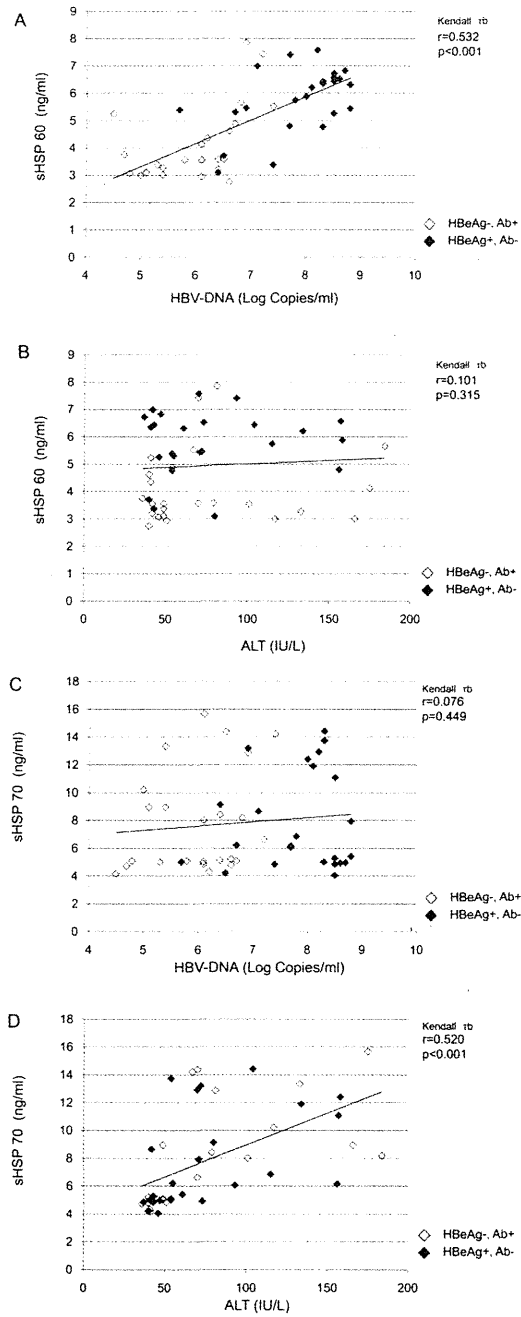
Figure 6. Analysis of the correlations between levels of heat shock proteins (HSPs), hepatitis B virus (HBV) DNA, and alanine aminotransferase (ALT). Open symbols indicate the values in samples from HBeAg-negative, HBeAb-positive patients. Filled symbols indicate the values in samples from HBeAg-positive, HBeAb-negative patients. The statistical analysis was performed by use of nonparametric Kendall τ_b methods. An approximately straight line is included in each graph. *A,* Correlation between heat shock protein 60 (HSP60) level and HBV DNA level. *B,* Correlation between HSP60 level and ALT level. *C,* Correlation between heat shock protein 70 (HSP70) level and HBV DNA level. *D,* Correlation between HSP70 level and ALT level.
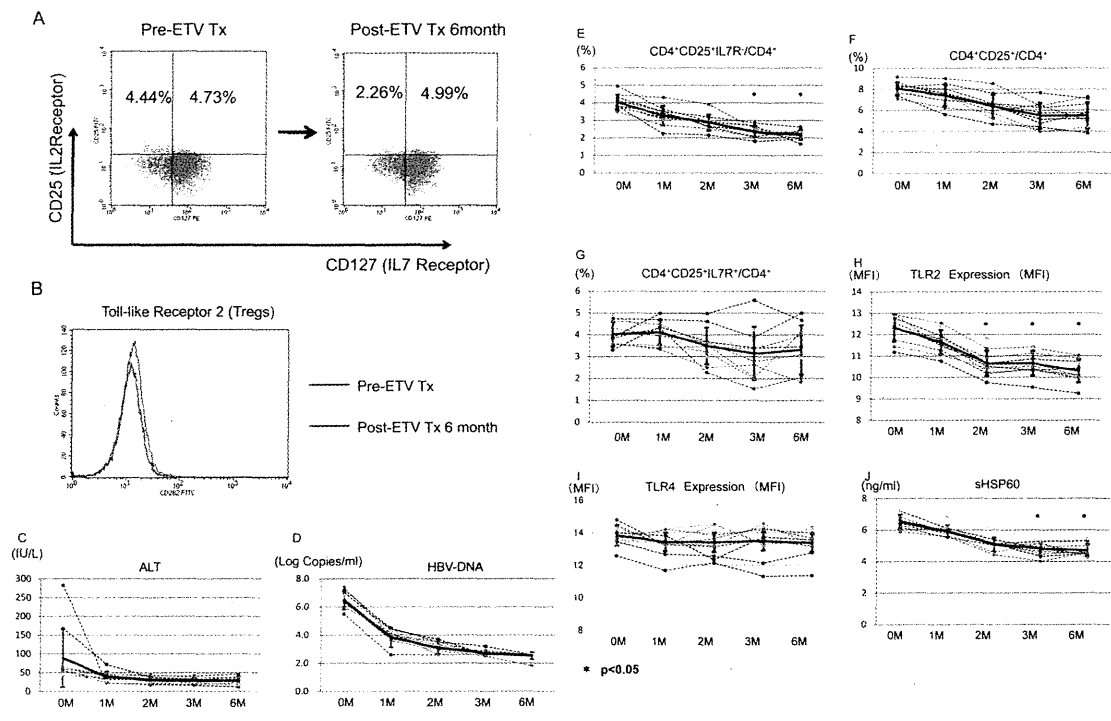
A

Pre-ETV Tx   Post-ETV Tx 6month

CD25 (IL2Receptor)

4.44%   4.73%   2.26%   4.99%

CD127 (IL7 Receptor)

B

Toll-like Receptor 2 (Tregs)

—— Pre-ETV Tx
—— Post-ETV Tx 6 month

C
(IU/L)

ALT

300
250
200
150
100
50
0

0M   1M   2M   3M   6M

D
(Log Copies/ml)

HBV-DNA

8.0
6.0
4.0
2.0
0.0

0M   1M   2M   3M   6M

E
(%)   CD4⁺CD25⁺IL7R⁻/CD4⁺

6
5
4
3
2
1
0

0M   1M   2M   3M   6M

F
(%)   CD4⁺CD25⁺/CD4⁺

10
8
6
4
2

0M   1M   2M   3M   6M

G
(%)   CD4⁺CD25⁺IL7R⁺/CD4⁺

6
5
4
3
2
1
0

0M   1M   2M   3M   6M

H
(MFI)   TLR2 Expression (MFI)

14
13
12
11
10
9
8

0M   1M   2M   3M   6M

I
(MFI)   TLR4 Expression (MFI)

16
14
12
10
8

0M   1M   2M   3M   6M

J
(ng/ml)   sHSP60

8
6
4
2
0

0M   1M   2M   3M   6M

* p<0.05

Figure 7. Sequential analysis of primary lymphocytes and soluble heat shock protein 60 (sHSP60) during entecavir (ETV) therapy. A, Representative dot plots of the CD4⁺CD25⁺IL7R⁻ cells before treatment and 6 months after the start of treatment. Peripheral blood mononuclear cells were stained with anti-CD3, anti-CD4, anti-CD25, and anti–IL7R (CD127). The phenotypes of the CD4⁺ cells were determined as follows: CD4⁺CD25⁺IL7R⁻ cells were identified as regulatory cells and CD4⁺CD25⁺IL7R⁺ cells were identified as activated CD4⁺ cells. B, Representative histogram of Toll-like receptor 2 (TLR2) surface expression on CD4⁺CD25⁺ regulatory T (T_reg) cells before treatment and 6 months after the start of treatment. C and D, Serum levels of alanine aminotransferase (ALT) and hepatitis B virus (HBV) DNA during ETV treatment. Solid black lines and error bars indicate the mean values and standard deviations, respectively. E–G, Frequencies of CD4⁺CD25⁺IL7R⁻cells, CD4⁺CD25⁺ cells, and CD4⁺CD25⁺IL7R⁺ cells among CD4⁺ cells during ETV treatment, respectively. H and I, Mean fluorescence intensity (MFI) of TLR2 and Toll-like receptor 4 (TLR4) expression on CD4⁺CD25⁺ cells during ETV treatment. J, Serum levels of sHSP60 during ETV treatment. *P < .01 for comparison between pretreatment levels and posttreatment levels.

Figure 8. Frequency of CD4⁺CD25⁺FoxP3⁺ cells.

$CD4^+CD25^+FoxP3^+$ cells was also decreased during lamivudine therapy. Moreover, the expression level of TLR2 on $CD4^+CD25^+$ cells gradually declined during entecavir therapy (Figure 7G).

Suppressive activity of T_{reg} cells. The suppressive activity of T_{reg} cells was analyzed by means of coincubation of unstained isolated T_{reg} cells and autologous $CD4^+CD25^-$ cells with CFSE staining. Ex vivo peripheral blood samples from 10 selected patients were analyzed before treatment, 3 months after the start of treatment, and 6 months after the start of treatment. The mean fluorescence intensity of the CFSE staining of the $CD4^+CD25^-$ cells was statistically significantly decreased at 6 months after the start of treatment ($P < .05$). These data indicate that the suppressive activity of T_{reg} cells was gradually decreased during entecavir treatment.

DISCUSSION

In this study, we have demonstrated that the levels of sHSP60 in patients with chronic hepatitis B were statistically significantly higher than those in patients with chronic hepatitis C. Moreover, the levels of sHSP60 were correlated with the HBV DNA levels but not with the ALT levels. On the other hand, the levels of sHSP70 were correlated with the ALT levels but not with the HBV DNA levels. This discrepancy in the correlation might be due to differences in the mechanism of heat shock protein production or secretion. The release of such heat shock proteins from cells is triggered by physical trauma and behavioral stress as well as by exposure to immunological danger signals [31, 32]. Stress protein release occurs both through physiological secretion mechanisms and during cell death by necrosis [33, 34]. HSP60 might be induced by the stress of HBV replication, because the levels of HSP60 were clearly correlated with the HBV DNA levels. On the other hand, HSP70 secretion might also be caused by cell death, because the levels of sHSP70 were correlated with the ALT levels. However, we should wait for more detailed studies about the HBV-specific induction of HSP60 to confirm this correlation. Extracellular stress proteins of the heat shock protein and glucose-regulated stress protein families, including HSP60, have powerful effects on the immune response [35]. Moreover, various kinds of immune cells such as macrophages, dendritic cells, $CD4^+$ effector T cells, and T_{reg} cells are affected by heat shock proteins [28, 35]. Most recently, Cohen-Sfady et al [36] reported that HSP60 enhanced the activity of IL-10 secretion from B cells. This effect could support our findings of the immune-suppressive effect of HSP60. However, we can not draw conclusions about the

whole effects of immune responses because the various kinds of immune cells might affect each other by means of cytokines, chemokines, stress-related proteins, and direct binding.

In this study, we focused on the effect of HSP60 on T_{reg} cell function by isolating T_{reg} cells, because many research groups had reported that the function and frequency of T_{reg} cells might be related to HBV replication. T_{reg} cells play an important role in the immune-hyporesponsiveness of patients with chronic hepatitis B. Previously, we demonstrated that the polarization of $CD4^+$ T cells was suppressed when the cells were stimulated with HBcAg in patients with chronic hepatitis B. T_{reg} cells are important cells in the suppression of the T helper 1 cell response by HBcAg, as demonstrated by the increased population of IL-10-secreting $CD4^+CD25^+$ cells. This indicates the presence of an inducible T_{reg} cell population, which is specific for HBcAg and produces IL-10, as well as a natural T_{reg} cell population in patients with chronic hepatitis B. Pretreatment with rHSP60 increased the frequency of HBcAg-specific IL-10-secreting $CD4^+CD25^+$ cells and enhanced the IL-10-secreting activity. These results indicate that pretreatment with rHSP60 might enhance the susceptibility of the HBcAg response and the function of IL-10 production by T_{reg} cells. These data might not imply that there was an expansion of HBcAg-specific T_{reg} cells as a result of the rHSP60 pretreatment, because the incubation phase was for only 16 h (4 h of pretreatment with rHSP60 plus 12 h of coincubation with HBcAg-presenting APCs). However, there is a possibility that continuous exposure to sHSP60 might induce an expansion of T_{reg} cells by enhancing the sensitivity of the expansion signal.

In this study, we found that the effect of HSP60 could be blocked by TLR2 neutralizing antibody but not by TLR4 neutralizing antibody. These data indicate that the effect of HSP60 could depend on TLR2. During entecavir therapy, not only the frequency of T_{reg} cells but also the serum levels of HSP60 and surface expression of TLR2 on T_{reg} cells gradually decreased. Therefore, we performed the suppression assay to detect the activity of T_{reg} cells by use of ex vivo isolated T_{reg} cells. The results of this suppression assay indicate that the reduction of the HBV DNA level could suppress the excessive activity of T_{reg} cells. In our previous study, the frequency and the function of HBV-specific cytotoxic T lymphocytes were partially recovered after therapy with nucleoside or nucleotide analogues [11]. The results clearly indicate that this restoration might be due to not only the reduction of HBV antigens but also the reduction of the frequency and function of T_{reg} cells.

On the basis of genomic analysis, 8 genotypes (A–H) of HBV have been defined, among which genotypes A, B, and especially C are prevalent in Japan [37–40]. Previous studies suggested that the clinical outcome of chronic hepatitis B was more severe in patients infected with genotype C, compared with those infected with genotype B [38, 39]. In this study, most of the

samples had HBV genotype C because of the high frequency of HBV genotype C infection in Japan. However, the expression levels of HSP60 were different among samples with the various genotypes in preliminary in vitro studies (data not shown). In addition, the expression patterns of chemokines in HBV-replicating Huh7 cells are apparently different among the various genotypes (Y. Kondo et al, unpublished data, May 2009). However, during entecavir treatment, the level of sHSP60 production in patients with genotype Bj HBV infection was quite similar to that in patients with genotype C HBV infection. We could not determine the relevance of the HBV genotypes and sHSP60 production levels because of the small numbers of genotype Bj–infected patients in this study.

In conclusion, we found that HSP60 was produced by HBV-replicating hepatocytes and determined the relevance of sHSP60 to T_{reg} cells functions, especially for IL-10-secreting activity. The understanding of the immunopathogensis of chronic hepatitis B could contribute to the development of novel kinds of immune therapy. Combination therapy with nucleoside or nucleotide analogues should be a reasonable method, because the suppression of HBV replication could reduce the excessive immune tolerance induced by T_{reg} cells.

References

1. Tiollais P, Pourcel C, Dejean A. The hepatitis B virus. Nature 1985; 317:489–495.
2. Lai CL, Ratziu V, Yuen MF, Poynard T. Viral hepatitis B. Lancet 2003; 362:2089–2094.
3. Kagi D, Ledermann B, Burki K, Zinkernagel RM, Hengartner H. Molecular mechanisms of lymphocyte-mediated cytotoxicity and their role in immunological protection and pathogenesis in vivo. Annu Rev Immunol 1996; 14:207–232.
4. Peng G, Li S, Wu W, Sun Z, Chen Y, Chen Z. Circulating CD4+ CD25+ regulatory T cells correlate with chronic hepatitis B infection. Immunology 2008; 123:57–65.
5. Barboza L, Salmen S, Goncalves L, et al. Antigen-induced regulatory T cells in HBV chronically infected patients. Virology 2007; 368:41–49.
6. Kondo Y, Ueno Y, Shimosegawa T. Immunopathogenesis of hepatitis B persistent infection: implications for immunotherapeutic strategies. Clin J Gastroenterol 2009; 2:71–79.
7. Xu D, Fu J, Jin L, et al. Circulating and liver resident CD4+CD25+ regulatory T cells actively influence the antiviral immune response and disease progression in patients with hepatitis B. J Immunol 2006; 177: 739–747.
8. Manigold T, Racanelli V. T-cell regulation by CD4 regulatory T cells during hepatitis B and C virus infections: facts and controversies. Lancet Infect Dis 2007; 7:804–813.
9. Kondo Y, Kobayashi K, Ueno Y, et al. Mechanism of T cell hyporesponsiveness to HBcAg is associated with regulatory T cells in chronic hepatitis B. World J Gastroenterol 2006; 12:4310–4317.
10. Kondo Y, Kobayashi K, Asabe S, et al. Vigorous response of cytotoxic T lymphocytes associated with systemic activation of CD8 T lymphocytes in fulminant hepatitis B. Liver Int 2004; 24:561–567.
11. Kondo Y, Asabe S, Kobayashi K, et al. Recovery of functional cytotoxic T lymphocytes during lamivudine therapy by acquiring multi-specificity. J Med Virol 2004; 74:425–433.
12. Chisari FV, Ferrari C. Hepatitis B virus immunopathogenesis. Annu Rev Immunol 1995; 13:29–60.
13. Reignat S, Webster GJ, Brown D, et al. Escaping high viral load exhaustion: CD8 cells with altered tetramer binding in chronic hepatitis B virus infection. J Exp Med 2002; 195:1089–1101.
14. Suri-Payer E, Amar AZ, Thornton AM, Shevach EM. CD4+CD25+ T cells inhibit both the induction and effector function of autoreactive T cells and represent a unique lineage of immunoregulatory cells. J Immunol 1998; 160:1212–1218.
15. Chen W, Jin W, Hardegen N, et al. Conversion of peripheral CD4+CD25− naive T cells to CD4+CD25+ regulatory T cells by TGF-beta induction of transcription factor Foxp3. J Exp Med 2003; 198:1875–1886.
16. Hori S, Nomura T, Sakaguchi S. Control of regulatory T cell development by the transcription factor Foxp3. Science 2003; 299:1057–1061.
17. Suvas S, Kumaraguru U, Pack CD, Lee S, Rouse BT. CD4+CD25+ T cells regulate virus-specific primary and memory CD8+ T cell responses. J Exp Med 2003; 198:889–901.
18. Nakamura K, Kitani A, Fuss I, et al. TGF-beta 1 plays an important role in the mechanism of CD4+CD25+ regulatory T cell activity in both humans and mice. J Immunol 2004; 172:834–842.
19. Zheng SG, Wang JH, Gray JD, Soucier H, Horwitz DA. Natural and induced CD4+CD25+ cells educate CD4+CD25− cells to develop suppressive activity: the role of IL-2, TGF-beta, and IL-10. J Immunol 2004; 172:5213–5221.
20. Sundstedt A, O'Neill EJ, Nicolson KS, Wraith DC. Role for IL-10 in suppression mediated by peptide-induced regulatory T cells in vivo. J Immunol 2003; 170:1240–1248.
21. Ulsenheimer A, Gerlach JT, Gruener NH, et al. Detection of functionally altered hepatitis C virus-specific CD4 T cells in acute and chronic hepatitis C. Hepatology. 2003; 37:1189–1198.
22. Marshall NA, Vickers MA, Barker RN. Regulatory T cells secreting IL-10 dominate the immune response to EBV latent membrane protein 1. J Immunol 2003; 170:6183–6189.
23. Beilharz MW, Sammels LM, Paun A, et al. Timed ablation of regulatory CD4+ T cells can prevent murine AIDS progression. J Immunol 2004; 172:4917–4925.
24. Wallin RP, Lundqvist A, More SH, von Bonin A, Kiessling R, Ljunggren HG. Heat-shock proteins as activators of the innate immune system. Trends Immunol 2002; 23:130–135.
25. Raz I, Elias D, Avron A, Tamir M, Metzger M, Cohen IR. Beta-cell function in new-onset type 1 diabetes and immunomodulation with a heat-shock protein peptide (DiaPep277): a randomised, double-blind, phase II trial. Lancet 2001; 358:1749–1753.
26. Hu W, Hasan A, Wilson A, et al. Experimental mucosal induction of uveitis with the 60-kDa heat shock protein-derived peptide 336–351. Eur J Immunol 1998; 28:2444–2455.
27. Mor F, Cohen IR. T cells in the lesion of experimental autoimmune encephalomyelitis: enrichment for reactivities to myelin basic protein and to heat shock proteins. J Clin Invest 1992; 90:2447–2455.
28. Zanin-Zhorov A, Cahalon L, Tal G, Margalit R, Lider O, Cohen IR. Heat shock protein 60 enhances CD4+ CD25+ regulatory T cell function via innate TLR2 signaling. J Clin Invest 2006; 116:2022–2032.
29. Sugiyama M, Tanaka Y, Kato T, et al. Influence of hepatitis B virus genotypes on the intra- and extracellular expression of viral DNA and antigens. Hepatology 2006; 44:915–924.
30. Inoue J, Takahashi M, Nishizawa T, et al. High prevalence of hepatitis delta virus infection detectable by enzyme immunoassay among apparently healthy individuals in Mongolia. J Med Virol 2005; 76:333–340.
31. Lindquist S, Craig EA. The heat-shock proteins. Annu Rev Genet 1988; 22:631–677.
32. Ellis RJ. The molecular chaperone concept. Semin Cell Biol 1990; 1: 1–9.
33. Hightower LE, Guidon PT Jr. Selective release from cultured mammalian cells of heat-shock (stress) proteins that resemble glia-axon transfer proteins. J Cell Physiol 1989; 138:257–266.
34. Mambula SS, Calderwood SK. Heat shock protein 70 is secreted from

tumor cells by a nonclassical pathway involving lysosomal endosomes. J Immunol 2006; 177:7849–7857.

35. Calderwood SK, Mambula SS, Gray PJ Jr, Theriault JR. Extracellular heat shock proteins in cell signaling. FEBS Lett 2007; 581:3689–3694.

36. Cohen-Sfady M, Pevsner-Fischer M, Margalit R, Cohen IR. Heat shock protein 60, via MyD88 innate signaling, protects B cells from apoptosis, spontaneous and induced. J Immunol 2009; 183:890–896.

37. Mahmood S, Niiyama G, Kamei A, et al. Influence of viral load and genotype in the progression of hepatitis B-associated liver cirrhosis to hepatocellular carcinoma. Liver Int 2005; 25:220–225.

38. Akuta N, Suzuki F, Kobayashi M, et al. Virological and biochemical relapse after discontinuation of lamivudine monotherapy for chronic hepatitis B in Japan: comparison with breakthrough hepatitis during long-term treatment. Intervirology 2005; 48:174–182.

39. Kobayashi M, Suzuki F, Akuta N, et al. Response to long-term lamivudine treatment in patients infected with hepatitis B virus genotypes A, B, and C. J Med Virol 2006; 78:1276–1283.

40. Tanaka Y, Mizokami M. Genetic diversity of hepatitis B virus as an important factor associated with differences in clinical outcomes. J Infect Dis 2007; 195:1–4.

Possible involvement and the mechanisms of excess *trans*-fatty acid consumption in severe NAFLD in mice

Noriyuki Obara[1], Koji Fukushima[1], Yoshiyuki Ueno[1,*], Yuta Wakui[1], Osamu Kimura[1], Keiichi Tamai[1], Eiji Kakazu[1], Jun Inoue[1], Yasuteru Kondo[1], Norihiko Ogawa[2], Kenta Sato[3], Tsuyoshi Tsuduki[3], Kazuyuki Ishida[4], Tooru Shimosegawa[1]

[1]Division of Gastroenterology, Tohoku University Graduate School of Medicine, 1-1 Seiryo, Aobaku, Sendai 980-8574, Japan; [2]Division of Advanced Surgical Science and Technology, Graduate School of Medicine, Tohoku University, Sendai, Japan; [3]Laboratory of Food and Biomolecular Science, Graduate School of Agricultural Science, Tohoku University, Sendai, Japan; [4]Department of Pathology, Tohoku University Hospital, Sendai, Japan

Background & Aims: Excessive *trans*-fatty acids (TFA) consumption has been thought to be a risk factor mainly for coronary artery diseases while less attention has been paid to liver disease. We aimed to clarify the impact of TFA-rich oil consumption on the hepatic pathophysiology compared to natural oil.
Methods: Mice were fed either a low-fat (LF) or high-fat (HF) diet made of either natural oil as control (LF-C or HF-C) or partially hydrogenated oil, TFA-rich oil (LF-T or HF-T) for 24 weeks. We evaluated the liver and body weight, serological features, liver lipid content and composition, liver histology and hepatic lipid metabolism-related gene expression profile. In addition, primary cultures of mice Kupffer cells (KCs) were evaluated for cytokine secretion and phagocytotic ability after incubation in *cis*- or *trans*-fatty acid-containing medium.
Results: The HF-T-fed mice showed significant increases of the liver and body weights, plasma alanine-aminotransferase, free fatty acid and hepatic triglyceride content compared to the HF-C group, whereas the LF-T group did not differ from the LF-C group. HF-T-fed mice developed severe steatosis, along with increased lipogenic gene expression and hepatic TFA accumulation. KCs showed increased tumor necrosis factor secretion and attenuated phagocytotic ability in the TFA-containing medium compared to its *cis*-isomer.

Conclusions: Excessive consumption of the TFA-rich oil up-regulated the lipogenic gene expression along with marked hepatic lipid accumulation. TFA might be pathogenic through causing severe steatosis and modulating the function of KCs. The quantity and composition of dietary lipids could be responsible for the pathogenesis of non-alcoholic steatohepatitis.

Introduction

In concordance with the prevalence of obesity, the incidence of non-alcoholic fatty liver disease (NAFLD) has increased and is nowadays recognized as the most common liver disease [2]. It is known that a part of NAFLD can progress to non-alcoholic steatohepatitis (NASH), liver fibrosis, cirrhosis and hepatocellular carcinoma [9]. Nevertheless, the mechanisms of NAFLD-to-NASH transition remain to be clarified; NAFLD appears to originate from the dysregulation of hepatic lipid metabolism as a part of the metabolic syndrome accompanied by visceral obesity, dyslipidemia, atherosclerosis, and insulin resistance [25]. According to the hypothetical theory named the 2-hit theory [5], the secondary hit to NAFLD that can be due to free fatty acid (FFA)s, oxidative stress, lipopolysaccharide (LPS) and inflammatory cytokines, causes NASH as a consequence.

In terms of the "first hit", the lipid accumulation in the liver is induced by high-fat diets [6,23] that include various lipid species. Such dietary lipid species uniquely affect the obesity phenotype, liver histology and gene expression pattern in the rat liver [3]. In this context, lipid species could play a potential role in the pathogenesis of NAFLD and/or NASH.

trans-Fatty acid (TFA) is produced through the industrial hardening of the vegetable oils to make the products more stable and robust, and thus easier to handle or store. Excess consumption of TFA is known as a risk factor for coronary artery diseases, insulin resistance and obesity accompanied by systemic inflammation, the features of metabolic syndrome [20,29]. Nevertheless, little is known about the effects on the liver induced by lipids.

Genetic and Metabolic Diseases

Research Article

Fast-foods, containing large amount of TFA in the form of margarine, spreads or frying oils, cause body-weight gain and abnormal serum alanine-aminotransferase (ALT) elevations in healthy subjects [15]. In addition, TFA-rich chow leads to hepatic steatosis [30], ALT elevations and insulin resistance in mice [17]; although the mechanisms have not been completely clarified. Therefore, we aimed to investigate the impact of the dietary lipid species and their quantities on the pathogenicity of hepatic inflammation and steatosis in mice. Comparing in particular natural oil and industrially produced partially hydrogenated TFA-rich oil of the same origin.

Materials and methods

Animal treatment

All the animal experiments were conducted under the approval of the Institutional Animal Care and Use Committees of Tohoku University. Female C57BL/6Njcl mice (8–10 weeks) were randomly assigned to four groups ($n = 6$ per group) and fed the designated chows (ORIENTAL YEAST Co. Ltd., Tokyo, Japan) ad libitum for 24 weeks, respectively. Low-fat diet (LF) and high-fat diet (HF) were made of either natural canola oil as control oil (LF-C and HF-C) or industry produced partially hydrogenated canola oil as TFA-rich oil (28.5% TFA/total fat, LF-T and HF-T), respectively (Table 1). After 12 h of fasting, the mice were sacrificed under diethylether anesthesia and the livers were removed and weighed. The divided livers were either stored at −80 °C for lipid, protein and gene expression analysis, or fixed in 4% paraformaldehyde and embedded in paraffin for histological evaluation. Standard chow-fed female C57BL/6Njcl mice (6–10 weeks) were used as a source of primary Kupffer cells (KCs).

Chemistry

Plasma aspartate-aminotransferase (AST), ALT, triglyceride (TG) and total cholesterol were measured with FUJI DRI-CHEM 7000 (FUJIFILM, Tokyo, Japan) at Biomedical Research Core of Tohoku University Graduate School of Medicine. Plasma adiponectin (AdipoGen, Seoul, Korea) and leptin (RayBio, GA, USA) were measured by Enzyme-Linked ImmunoSorbent Assay (ELISA). Plasma FFA, high density lipoprotein (HDL)-cholesterol and (very) low density lipoprotein ((V)LDL)-cholesterol were measured by enzymatic assay kits (BioVision, CA, USA).

Histology and immunohistochemistry

The thin-sliced specimens were stained with hematoxylin and eosin to evaluate steatosis and inflammation or Sirius red to evaluate fibrosis of the liver. The histology was scored by the NAFLD activity score (NAS) [16]. KCs were stained with anti-F4/80 monoclonal antibody (Abcam, Cambridge, UK) and neutrophils were detected by myeroperoxidase immunostaining (Abcam). Apoptosis was evaluated by TUNEL method using an ApopTag kit (Chemicon, CA, USA).

Immunoblot analysis and real-time RT-PCR

Liver protein extracts were evaluated by immunoblot analysis with the following primary antibodies: phosphor-AKT (Thr308 and Ser473), total AKT (Cell Signaling Technology, Danvers, MA) and β-actin (Sigma, MO, USA). RNA extracted from the livers was subjected to real-time RT-PCR analysis using the specifically designed primer sets purchased form TAKARA BIO Perfect Real Time Support System (TAKARA BIO INC., Tokyo, Japan) and One Step SYBR Prime Script RT-PCR Kit II (TAKARA BIO INC.), and only PGC-1β was analyzed using the specifically designed TaqMan primer set and 1-step kit (Applied Biosystems, CA, USA). All results were normalized by GAPDH as the internal control.

Lipidomic analysis of the liver

Hepatic TG and FFA content were measured by enzymatic assay kit (BioVision) and were normalized by the liver weight. Hepatic lipid peroxide was evaluated by measuring TBARS (thiobarbituric acid reactive substances, Cayman Chemical Company, USA) in the liver and was normalized by the protein level [18]. Total lipids from the liver were extracted by Folch's procedure [10]. The lipids were methylated and evaluated by gas chromatography as previously reported [31].

Isolation and culture of primary Kupffer cells

KCs were isolated as reported previously [28]. Briefly, the mice livers were digested by two-step collagenase perfusion. The minced livers were subjected to the gradient centrifugation of Percoll (Sigma) and succeeding counterflow centrifugal elutriation. The viabilities of the obtained cells evaluated by trypan blue staining were more than 85%, and the purity was more than 90% determined by the population of CD11b positive cells counted by FACS Calibur (Becton Dickinson, Tokyo, Japan). KCs were suspended in RPMI1640 medium with 10% fetal bovine serum and antibiotics (100 U/ml penicillin G, 100 μg/ml streptomycin sulfate) and incubated overnight at 37 °C in 5% CO_2 incubator for the succeeding examinations.

Fatty acid treatment

Fatty acids (Larodan Fine Chemicals, Malmo, Sweden) were dissolved in RPMI1640 medium with 1% fatty acid-free bovine serum albumin (Calbiochem, Darmstadt, Germany) and adjusted to a final concentration of 200 μM with 1% bovine serum albumin, 1% ITS-A supplement (GIBCO, CA, USA) and antibiotics same as above. After overnight incubation, KCs were washed and the medium was changed to fatty acid-containing medium or fatty acid-free medium as the control, and incubated for another 24 h.

Cytokine production by KCs stimulated with lipopolysaccharide

After 24 h incubation, KCs were stimulated by LPS (100 ng/ml, SIGMA) combined with LPS-binding protein (200 pg/ml, ALEXIS BIOCHEMICALS, Lausanne, Switzerland) for 6 h, and the cell viability was determined by MTS assay (3-(4,5-dimethylthiazol-2-yl)-5-(3-carboxymethoxyphenyl)-2-(4-sulfophenyl)-2H-tetrazolium, inner salt and phenazine ethosulfate, Promega, Tokyo, Japan). The supernatants were subjected to ELISA (Thermo Fisher Scientific Inc., IL, USA) for the evaluation of the tumor necrosis factor-alfa (TNFα) and interleukin-6 (IL-6) production.

Phagocytotic ability of KCs

After 24 h incubation, KCs were incubated at 37 °C for 1 h with 1 μm latex beads (75 ng/ml, SIGMA) or at 4 °C in the fatty acid-free medium as control. After incubation, the cells were washed 3 times, detached with trypsin/EDTA and analyzed by FACS calibur [1].

Statistical analysis

The results are shown as the mean ± standard deviation (SD), and were analyzed by SPSS software (SPSS INC., Tokyo, Japan).

The differences between the groups were tested by ANOVA, followed by Tukey post hoc test. A p values less than 0.05 were considered statistically significant.

Table 1. Diet compositions.

	Low-fat diet		High-fat diet	
	Control oil (LF-C) kcal%	TEA-rich oil (LF-T) kcal%	Control (HF-C) kcal%	TEA-rich (HF-T) kcal%
Diet compositions				
Protein	13.8	13.8	18.8	18.8
Carbohydrate	74.4	74.4	17.6	17.6
Over all fat	11.8	11.8	63.6	63.6
Fat composition (g/100 g)				
Saturated	7.8	21.7	7.8	21.7
(cis-)Monounsaturated	62.5	45.3	62.5	45.3
Polyunsaturated	29.7	4.5	29.7	4.5
trans- (%)		28.5		28.5

Results

Physiological and biochemical characteristics

Body weight was similar between LF-fed mice, increased in HF-fed mice compared to LF-fed mice, and strikingly HF-T-fed mice weighed 1.3-fold more than HF-C-fed mice (Table 2). Liver weight was significantly increased in only HF-T-fed mice by approximately 2-fold compared to the other groups. The liver–body weight ratio was significantly increased by 1.2- and 1.6-fold in LF-T-fed and HF-T-fed mice, respectively, compared to the corresponding control groups with the same dietary composition, and decreased by approximately 20% in the HF-C-fed mice compared to the LF-C-fed mice.

Plasma AST, ALT, TG, FFA and leptin were similar between the LF groups irrespective of the dietary lipid source, but in the LF-T group, total cholesterol, HDL-cholesterol, (V)LDL-cholesterol and adiponectin were significantly decreased compared to the LF-C group (Table 2). In contrast, some serum markers were elevated in the HF-T group compared to the HF-C group, particularly AST, ALT, TG, total cholesterol, (V)LDL-cholesterol, FFA and leptin were significantly increased. As for the control oil-fed mice, total cholesterol, HDL-cholesterol, (V)LDL-cholesterol and adiponectin were lower, whereas plasma leptin was higher in HF-C-fed than in LF-C-fed mice. Between TFA-rich oil-fed mice, all serum markers except adiponectin were also significantly higher in HF-T-fed than in LF-T-fed mice.

Liver histology

There were few lipid droplets in LF-C-fed mice liver. Mild microvesicular and macrovesicular steatosis was present around zone 1 in LF-T-fed mice livers and abundant large lipid droplets around zones 1 and 2 in HF-C-fed mice livers. Inflammation and ballooning degeneration were minimal in these groups (Fig. 1A). However, the HF-T-fed mice livers were characterized by foamy, prominent microvesicular steatosis throughout the lobe and some macrovesicular lipid droplets in zones 1 and 2. Most of the hepatocytes were expanded with marked small lipid droplets that surrounded the nuclei, and the severely expanded hepatocytes presented the phenotype of ballooning degeneration (Fig. 1A); moreover, some of the fatty hepatocytes were surrounded by infiltrated neutrophils confirmed by immunostaining for myeloperoxidase, forming lipogranuloma (Fig. 1B) accompanied by ballooning hepatocytes (Fig. 1C). The number of neutrophils was increased in HF-T-fed mice livers (Fig. 1D). However, when evaluated by NAS, the HF-T group did not show significant differences (Table 2).

To investigate the involvement of KCs in the pathological difference between the HF-C group and HF-T group, we performed immunohistochemical staining for F4/80, a macrophage-restricted surface glycoprotein. F4/80-positive cells were more prevalent in the HF-T group (Fig. 1E). Although fibrosis was not identified visually by Sirius red staining in any of the groups (not shown), collagen type1, α1 mRNA expression in the liver, as an early fibrosis marker, increased only in HF-T-fed mice by 3.6-fold compared to LF-C-fed mice (Fig. 1F). TUNEL assay did not reveal conspicuous apoptotic hepatocytes in each group, however some non-parenchymal cells were TUNEL positive (Supplementary Fig. 1).

Lipid and lipid peroxide content and fatty acid composition of liver

The hepatic total lipid (Fig. 2A), TG (Fig. 2B), FFA (Fig. 2C) and lipid peroxide contents (Fig. 2D) did not differ between the LF-C and LF-T groups. On the other hand, reflecting the marked liver weight gain and histological steatotic changes, hepatic total lipid, TG and lipid peroxide content were significantly increased in the HF-T group compared to the HF-C group, while FFA content did not differ. All of these markers had a tendency to be elevated in the HF groups compared to the LF groups and when compared between the corresponding dietary oil-fed groups, although the TG increase in HF-C-fed mice was not statistically significant.

Table 2. Influence of *trans*-fatty acid-rich oil intake for the physiological and biochemical characteristics.

	Low-fat diet		High-fat diet	
	Control oil (LF-C)	TFA-rich oil (LF-T)	Control oil (HF-C)	TFA-rich oil (HF-T)
Body weight (g)	24.4 ± 2.1	23.1 ± 1.3	31.8 ± 3.6$^\sharp$	40.9 ± 7.0$^{*\sharp\dagger}$
Liver weight (g)	1.08 ± 0.16	1.22 ± 0.08	1.11 ± 0.11	2.40 ± 1.01$^{*\sharp\dagger}$
Liver–body weight ratio (%)	4.5 ± 0.4	5.4 ± 0.2*	3.5 ± 0.3$^\sharp$	5.6 ± 1.6*†
Plasma characteristics				
Aspartate-aminotransferase (IU/L)	95.2 ± 12.4	82.5 ± 20.8	136.8 ± 47.0	262.2 ± 72.0$^{*\sharp\dagger}$
Alanine-aminotransferase (IU/L)	48.8 ± 15.0	37.0 ± 7.3	50.4 ± 10.9	244.0 ± 105.7$^{*\sharp\dagger}$
Triglyceride (mg/dl)	60.3 ± 19.2	51.0 ± 12.8	62.4 ± 14.8	124.8 ± 45.0$^{*\sharp\dagger}$
Total cholesterol (mg/dl)	77.0 ± 8.9	47.5 ± 6.1*	55.2 ± 5.0	87.8 ± 10.1$^{*\sharp}$
HDL-cholesterol (mg/dl)	51.6 ± 8.3	26.2 ± 3.9*	33.3 ± 7.2$^\sharp$	38.6 ± 5.0$^{\sharp\dagger}$
(V)LDL-cholesterol (mg/dl)	16.8 ± 2.1	12.0 ± 1.5*	11.9 ± 1.0$^\sharp$	17.4 ± 1.7$^{*\sharp}$
Free fatty acids (nmol/ml)	1.77 ± 0.38	1.43 ± 0.31	1.99 ± 0.58	3.64 ± 0.42$^{*\sharp\dagger}$
Adiponectin (μg/ml)	25.5 ± 1.4	18.2 ± 1.4*	20.0 ± 1.5$^\sharp$	20.0 ± 1.4†
Leptin (ng/L)	5.6 ± 0.7	5.3 ± 0.6	13.8 ± 2.0$^\sharp$	23.7 ± 2.3$^{*\sharp\dagger}$
Total: HDL-cholesterol ratio	1.54 ± 0.06	2.33 ± 0.5*	1.71 ± 0.37	2.25 ± 0.87†
NAFLD activity score				
Steatosis	0.33 ± 0.52	0.17 ± 0.41	1.67 ± 0.82$^\sharp$	1.17 ± 0.41$^\sharp$
Inflammation	0.33 ± 0.52	0.33 ± 0.52	0.83 ± 0.75	1.00 ± 0.63
Ballooning	0.00 ± 0.00	1.00 ± 0.63*	1.00 ± 0.00$^\sharp$	1.67 ± 0.82†

All values are means ± SD (*n* = 6 per each group).
* Significantly different from the corresponding control group with the same dietary composition; $p < 0.05$.
$^\sharp$ Significantly different from the low-fat diet with the same dietary lipid as a source; $p < 0.05$.
† Significantly different from low-fat control diet group; $p < 0.05$.

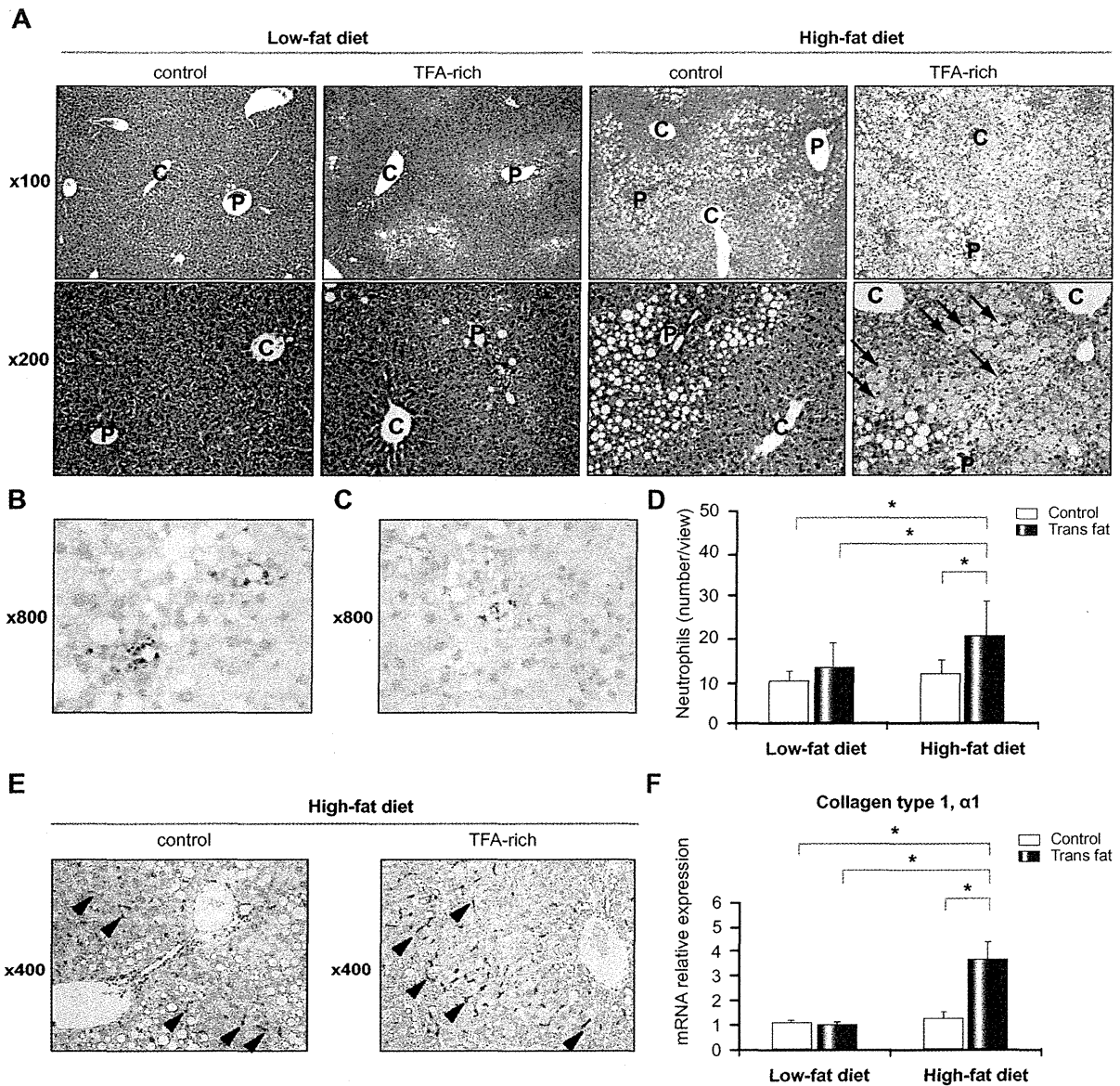# Research Article

A

B

C

D

E

F

Fig. 1. Distinct steatotic features of the liver. (A) Representative liver histology stained with H&E. Remarkably expanded hepatocytes with extensive small lipid droplets make a feature of ballooning degeneration (arrows). Neutrophils confirmed by myeloperoxidase staining were (B) forming lipogranulomas and (C) surrounding the ballooning degenerated hepatocytes. (D) The number of neutrophils is increased in HF-T-fed mice liver. (E) KCs were detected by anti-F4/80 immunohistochemical staining (arrow heads). (F) Quantitative RT-PCR revealed elevation of collagen type 1, $\alpha1$ mRNA expression in liver of HF-T-fed mice. P, portal tract; C, central vein. *$p < 0.05$.

We evaluated the lipid composition of the liver to examine the pathological condition in the model. Compared to the LF-C group, the sum of total polyunsaturated fatty acid (PUFA), n-6 PUFA and n-3 PUFA was decreased in the LF-T group, but did not differ significantly in the other groups (Fig. 2E.). In the HF-C group, the sum of saturated fatty acid (SFA) and monounsaturated fatty acid (MUFA) was decreased, and total PUFA, n-6 PUFA and n-3 PUFA were increased compared to the LF-C group. However, in the HF-T group, total PUFA and n-6 PUFA decreased significantly compared to the LF-C group, and their proportions were similar to those of the LF-T group. The potentially beneficial lipid n-3

PUFA that is thought to prevent insulin resistance and hepatic steatosis [11], was increased even in the HF-T group compared to the LF-T group, the level of which was similar to that of the LF-C group.

The content of individual fatty acids in the liver coordinated nearly synergistically with the sum of the content of the fatty acids in the same unsaturation grade (Fig. 2E and Table 3). The unique accumulation of elaidic acid (18:1(9-$trans$)), chief component of dietary TFA, was noteworthy in the LF-T and HF-T groups. The content of arachidonic acid (20:4n-6) alone decreased to 70% only in the HF-T group, which was similar to the LF-T group in